

University of Texas Rio Grande Valley

**ScholarWorks @ UTRGV**

---

Mechanical Engineering Faculty Publications  
and Presentations

College of Engineering and Computer Science

---

6-10-2015

## **Fatigue Life Estimation of Modified Railroad Bearing Adapters for Onboard Monitoring Applications**

Alexis Trevino

Arturo A. Fuentes

Constantine Tarawneh

Joseph Montalvo

Follow this and additional works at: [https://scholarworks.utrgv.edu/me\\_fac](https://scholarworks.utrgv.edu/me_fac)



Part of the [Mechanical Engineering Commons](#)

---

**JRC2015-5790**

**FATIGUE LIFE ESTIMATION OF MODIFIED RAILROAD BEARING ADAPTERS FOR ONBOARD MONITORING APPLICATIONS**

**Alexis Trevino**

Mechanical Engineering Department  
The University of Texas-Pan American  
Edinburg, Texas, USA

**Arturo A. Fuentes, Ph.D.**

Mechanical Engineering Department  
The University of Texas-Pan American  
Edinburg, Texas, USA

**Constantine M. Tarawneh, Ph.D.**

Mechanical Engineering Department  
The University of Texas-Pan American  
Edinburg, Texas, USA

**Joseph Montalvo**

Mechanical Engineering Department  
The University of Texas-Pan American  
Edinburg, Texas, USA

**ABSTRACT**

This paper presents a study of the fatigue life (i.e. number of stress cycles before failure) of Class K cast iron conventional and modified railroad bearing adapters for onboard monitoring applications under different operational conditions based on experimentally validated Finite Element Analysis (FEA) stress results. Currently, freight railcars rely heavily on wayside hot-box detectors (HBDs) at strategic intervals to record bearing cup temperatures as the train passes at specified velocities. Hence, most temperature measurements are limited to certain physical railroad locations. This limitation gave way for an optimized sensor that could potentially deliver significant insight on continuous bearing temperature conditions. Bearing adapter modifications (i.e. cut-outs) were required to house the developed temperature sensor which will be used for onboard monitoring applications. Therefore, it is necessary to determine the reliability of the *modified* railroad bearing adapter. Previous work done at the University Transportation Center for Railway Safety (UTCRS) led to the development of finite element model with experimentally validated boundary conditions which was utilized to obtain stress distribution maps of conventional and modified railroad bearing adapters under different service conditions. These maps were useful for identifying areas of interest for an eventual inspection of railroad bearing adapters in the field. Upon further examination of the previously acquired results, it was

determined that one possible mode of adapter failure would be by fatigue due to the cyclic loading and the range of stresses in the railroad bearing adapters. In this study, the authors experimentally validate the FEA stress results and investigate the fatigue life of the adapters under different extreme case scenarios for the bearing adapters including the effect of a railroad flat wheel. In this case, the flat wheel translates into a periodic impact load on the bearing adapter. The Stress-Life approach is used to calculate the life of the railroad bearing adapters made out of cast iron and subjected to cyclic loading. From the known material properties of the adapter (cast iron), the operational life is estimated with a mathematical relationship. The Goodman correction factor is used in these life prediction calculations in order to take into account the mean stresses experienced by these adapters. The work shows that the adapters have infinite life in all studied cases.

**INTRODUCTION**

One of the major goals of the University Transportation Center for Railway Safety (UTCRS) is to increase the railway reliability by, among other things, developing advanced technology for infrastructure monitoring and developing innovative safety assessments and decision-making tools. Along these lines, the Railroad Research Group at the University of Texas-Pan American has been working on

onboard monitoring systems for the railroad industry. Currently, to identify distressed bearings in service, the railroad industry employs monitoring equipment to warn of impending failures. The conventional method is to place wayside hot-box detectors (HBDs) at strategic intervals to record bearing cup temperatures as the train passes at specified velocities. HBDs take a snapshot of the bearing temperature at designated wayside detection sites which may be spaced as far apart as 65 km (~40 mi). HBDs are designed to identify those bearings which are operating at temperatures greater than 93.4°C (170°F) above ambient conditions. An extension to the current practice is to track the temperature of each bearing and compare it to the average temperature of all bearings from the same side of the train. Thus, bearings that are “trending” above normal can be identified and tracked without waiting for a hot-box detector to be triggered [1]. Future technologies are focusing on continuous temperature tracking of railroad bearings (e.g. IONX motes) [2]. Since placing sensors directly on the bearing cup is not feasible due to cup indexing during service, the next logical location for such sensors (e.g. IONX motes) is the bearing adapter. The railroad bearing assembly adapter acts as a medium between the axle assembly (bearings, wheels) and the side frame, as can be seen in Figure 1. Modifications (e.g. cutouts) were necessary in order to house the temperature sensor and integrated circuit on the bearing adapter.

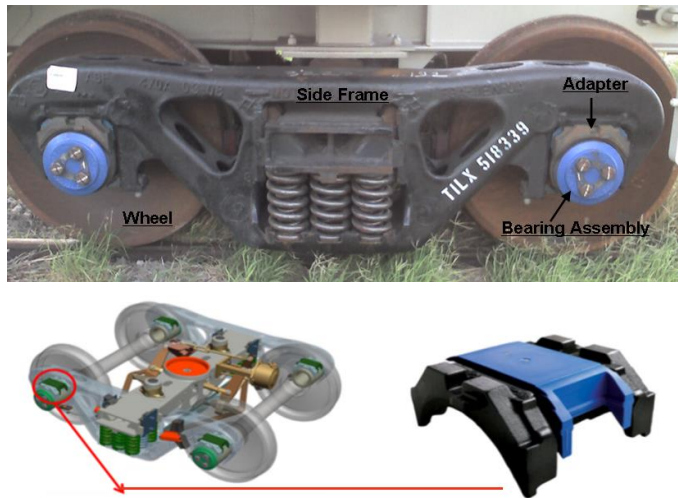


**Figure 1: Railcar Truck Assembly and Railroad Bearing AdapterPlus with Elastomer Pad-Liner**  
[Schematics are courtesy of Amsted Rail Company, Inc. ([www.amstedrail.com](http://www.amstedrail.com))]

The temperature sensor is embedded in the bearing adapter between the Adapter Plus™ Pad and the railroad bearing. Original railroad bearing adapters have gone through modification to house the sensor. The modifications to the railroad bearing adapters include the removal of material to accommodate the sensor. Figures 2 and 3 show, respectively, the non-modified and modified bearing adapters without the elastomer pad-liner and sensor.

Previous work done by the UTCRS found the stress distributions on bearing adapters with normal and some abnormal boundary conditions in the top and bottom interfaces with the elastomer pad-liner and the bearing, respectively [3].

It is important to know the stress maps in order to know certain points of interest to inspect, in which the part may fail. The objective of this paper is to estimate the fatigue life of the bearing adapter at certain loading conditions. It is imperative to know the life of the adapter in order to know when to take it out from service and prevent catastrophic failure.

The main purpose of this work is to estimate the fatigue life of the adapters with several expected boundary conditions, including worst case conditions, and to compare the life between the original adapter and the modified adapter. This will be done using the stress-life approach with the Goodman correction factor to take into account the effect of mean stresses in these parts.



**Figure 2: Original Railroad Bearing AdapterPlus™ without Elastomer Pad-Liner**

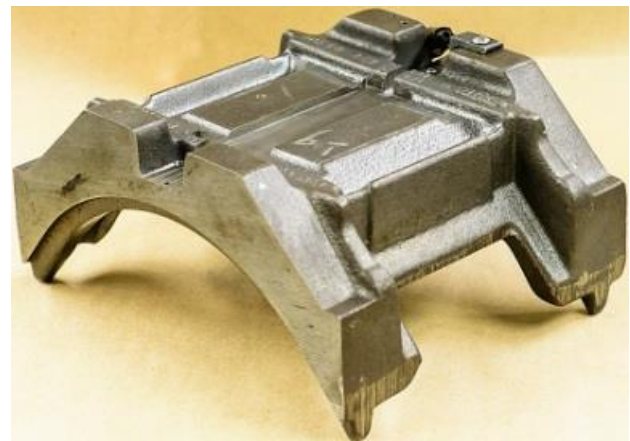


**Figure 3: Modified Railroad Bearing AdapterPlus™ without Elastomer Pad-Liner**

## PREVIOUS WORK/METHODOLOGY

This section discusses the methodology used to obtain the fatigue life of the bearing adapters. First, a previous experimentally informed FEA for modified bearing adapters under certain loading scenarios by Montalvo et al. [3] is presented. Then, an expected worst case scenario that would be used to obtain the fatigue results was established. The selected worst case scenario was the case of the train having a

wheel flat; which translates into a periodic impact load on the flat wheel which translated to a periodic impact loading on the bearing adapter. Finally, the previous experimentally informed FEA results were updated and utilized to estimate the operational life of the adapters using the Stress-Life approach.

Previous FEA Work

Previous work done by Montalvo et al. [3] was reviewed and expanded to get the expected maximum stresses at points of interest; these results were necessary to determine the number of cycles a bearing adapter will be able to withstand. In the previous work, the stress distribution for Class E and Class K Railroad Bearing Adapters under full load was determined using Finite Element Analysis. Experimentally informed conditions were used in order to model the bearing adapters shown in Figure 4. Laboratory experiments involving the use of pressure films were conducted in order to determine the appropriate boundary conditions experienced by the bearing adapter. Values for the contact pressure between the bearing cup and the adapter and between the elastomer pad-liner and the adapter were obtained for the AdapterPlus™ Class K based on the pressure film experiments.

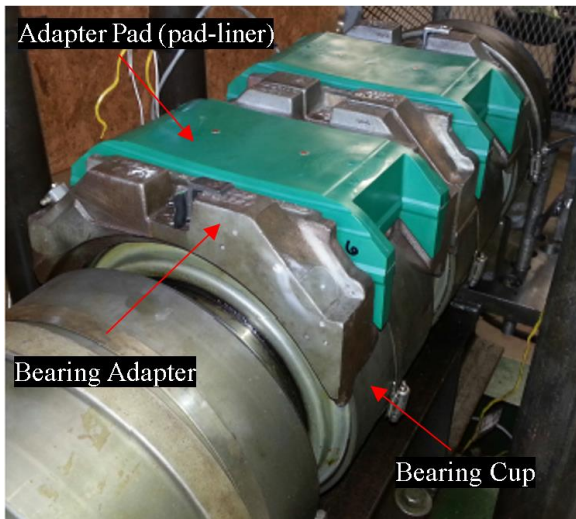


**Figure 4: Railroad Bearing Cup, Adapter and Pad**

A radial constraint was applied at the bottom rounded surface of the adapter (e.g. bottom contact length of 4 or 6 inches), and a pressure was applied at the top surface of the adapter (e.g. 1,375 psi). Figure 5 shows the boundary conditions of one of the models while Figure 6 shows sample result of the bearing adapter. Details of the boundary conditions, FEA and convergence of results can be found in the work by Montalvo et al. [3].

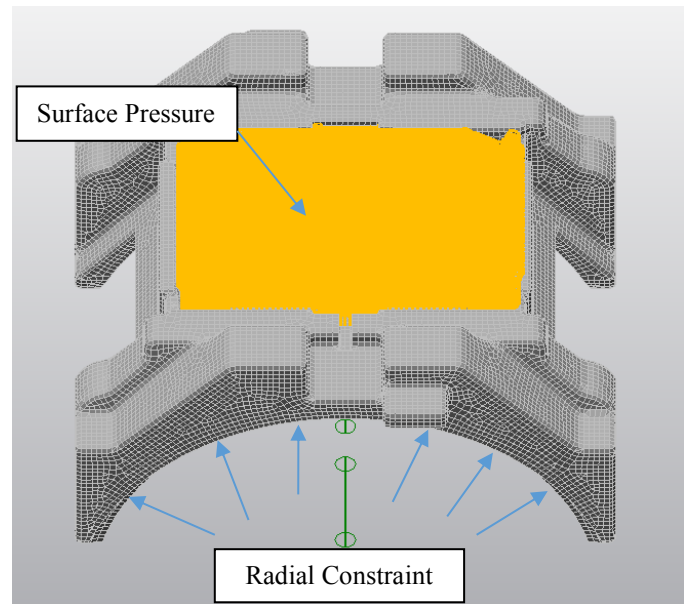


**Figure 5: Boundary Conditions for FEA**

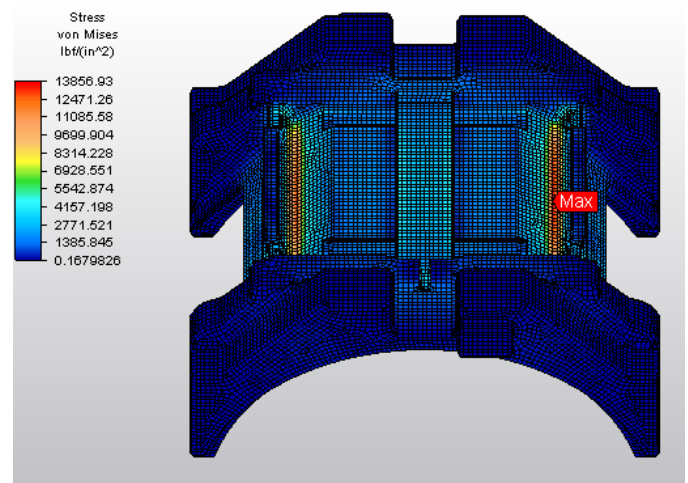


**Figure 6: Sample FEA Stress Result for Class K Modified Adapter**

Impact Load

In order to determine one of the possible worst case scenarios for the bearing adapter, the impact load experienced by a railroad wheel was studied. Previous work dealt with obtaining FEA stress distributions for bearing adapters under full static load. However, it was of interest to determine the stress maps of the bearing adapters under a dynamic (or impact load) caused by flat wheels. In this section, it is first described how the impact load on bearing adapters is obtained and how it will be used to determine fatigue life. Subsequently, the number of cycles for a flat wheel development and removal is estimated to have an idea of how long the bearing adapter will operate under these conditions.

The difference between a static load and a dynamic load can be very significant. A static load would be equivalent to wheel or bearing adapter operating at a full load of 35,750

lb; while a dynamic load would be the wheel experiencing an impact due to a wheel flat during operation. Previous research done by Stratman et al. [4] illustrates the load experienced by operating wheels sensed by wheel impact load detectors (WILDs). WILDs detect the load experienced by a wheel at certain physical locations. It is mentioned that the wheel impact load limit allowed by the Association of American Railroads (AAR) is 403 kN (90,000 lb), at which wheels are usually removed. This load is translated to a wheel or bearing in cases like flat wheels. For this paper, it is assumed that the highest static equivalent load experienced by a wheel would be approximately 90,000 lb. Therefore, the selected worst case scenario for this fatigue study was of a wheel under almost three times the full static load (i.e. impact loading). The previous FEA results obtained by Montalvo et al. only included the bearing adapters at full static load. Thus, these results were updated to include the FEA results for a bearing adapter under impact loading (i.e. equivalent static load of 90,000 lb) which would be used to determine the number of operational cycles.

In order to get an idea of how long railroad bearing adapter will be subjected to these operating conditions, information for the mileage of high impact wheels was found in the literature [4] and is provided in Table 1.

**Table 1: Life Mileage of High Impact Railroad Wheels**

	<b>Mileage from wheel mount date until deviation from average impact, km</b>	<b>Mileage from average dynamic to peak impact, km</b>	<b>Total mileage from wheel mount date until peak impact, km</b>
<b>High-impact wheels</b>	573,000.5	43,240.5	636,906.1

From Table 1, an estimate of the life of the wheels in cycles or revolutions can be obtained through a simple calculation. The number of cycles that the railroad wheel will experience impact loading can be calculated using the following relationship:

$$Life_{Wheel} = \frac{Mileage}{Perimeter} = \frac{Mileage}{\pi \times Diameter} \quad (\text{cycles or rev.}) \quad (1)$$

where the life is the number of cycles by the wheel, mileage is the distance traveled by the train, and the diameter is the one for the railroad wheel. For example, assuming a mileage of 636,906.1 km or 395,839.7 mi and a wheel diameter of 3 ft, using Equation (1), the wheel life is estimated to be  $2.2 \times 10^8$  cycles.

The number of cycles that the bearing adapter will experience impact loading can be estimated to be the same as the life of the wheel above. This estimation can be related to a distance or time of operation, depending on the velocity of the train.

## Fatigue Life

In this section, a brief description of the Stress-Life approach is given and discussed. Afterwards, the effect of mean stresses is explained along with the Goodman modifying factor. Subsequently, the assumptions made for the fatigue life estimation are stated and explained.

### *Stress-Life Approach*

A detailed explanation of the Stress-Life approach can be found in the work by Stephens et al. [5]. The stress-life method is one of the most common methods for determining the life of metal components. This method has its origins from the work of Wohler in the 1850s. The way this method works is by obtaining the SN-curves for certain materials by performing experiments or tests. SN curves give a relationship between stress amplitude and number of cycles to failure.

Tests are conducted in order to obtain the bending and axial properties of materials. These experiments consist of loading certain material specimens cyclically until the parts fail. The experiments are repeated at different loads; and the values for the load (or stress) are plotted versus the number of cycles. There are two significant points in SN curves: the endurance limit ( $S_{FL}$ ) and the low cycle stress value ( $S_F$ ). These values can be estimated to a multiple of the ultimate tensile strength, depending on how the part is loaded. Subsequently, the stress-life properties of each material at each loading scenario can be obtained and the stress life can be estimated.

The Fatigue Limit or Endurance Limit,  $S_{FL}$  is the stress below which failures will not occur in laboratory. This is considered to be a safe stress level. Usually, the fatigue limit of materials can be predicted or estimated from the tensile property of the specific material.

### *Mean Stresses*

It is known that compressive stresses increase the life of a component or part, while tensile stresses decrease the number of cycles or life of a part. In order to account for these effects, correction factors were needed. The most common correction factor is the Goodman, which was proposed in 1890. For this study, the points of interest in the adapter were in tension, therefore, it is important to take into account the mean stresses.

The fatigue limit for zero mean stress is plotted on one axis and the ultimate strength on the other, as shown in Figure 7. Then, the mean stress and alternating stress amplitude are obtained at the studied case. Afterwards, to find an equivalent stress in this line, a point is created on the graph from the respective mean stress and alternating stress amplitude. A line is created through this point and the  $UTS$  as shown in red in Figure 7. Finally, the equivalent stress amplitude can be obtained for any material in the vertical axis using Equation (2).



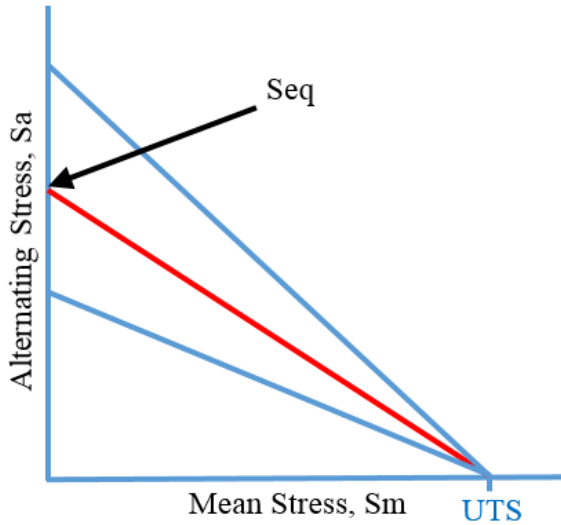


**Figure 7: Goodman Diagram**

The diagram can be described by:

$$\frac{S_a}{S_{eq}} + \frac{S_m}{UTS} = 1 \quad (2)$$

where  $S_{eq}$  is the equivalent stress,  $UTS$  is the ultimate tensile strength of the material. Similarly,  $S_a$  is the alternating stress or stress amplitude while  $S_m$  is the mean stress and are defined as:

$$S_m = \frac{S_{max} + S_{min}}{2} \quad (3)$$

$$S_a = \frac{S_{max} - S_{min}}{2} \quad (4)$$

#### *Fatigue Estimation Assumptions*

In this paper, the fatigue life of cast iron bearing adapters under impact loading was studied. The main purpose was to determine the life of these components and if removal of material will affect significantly the integrity of the bearing adapters. The bearing adapter is made of Iron-Ductile 60-14-18. The properties: density of  $\rho = 6.65 \times 10^{-4} \text{ lbf} \cdot \text{s}^2 / \text{in}^3$ , a modulus of elasticity of  $E = 23 \times 10^6 \text{ psi}$ , ultimate tensile strength  $UTS = 60,000 \text{ lb}$  and a Poisson's ratio of  $\nu = 0.275$ , were used for the bearing adapter. Specifically, the endurance limit for iron is:

$$S_{FL}(\text{iron}) \cong 0.4 \times UTS = 24 \text{ ksi} \quad (5)$$

From the previously made assumptions of a flat wheel translating into an equivalent static load of 90,000 lb, FEA impact loading results for the conventional and modified bearing adapters were obtained based on the work done by Montalvo et al. [3].

The worst case stresses used to determine the fatigue results are based on the assumption that the conventional and modified bearing adapters are fully loaded and unloaded in one cycle. The partial unloading of the bearing adapter will decrease the equivalent stress. Thus, it will increase the adapter life (i.e. stress cycles). In the fatigue life results in this

study, the assumption was that the maximum load was 90,000 lb and the minimum load was 0 lb. The mean stress and alternating stress amplitude was obtained using Equations (3) and (4), while the equivalent stress was obtained using the Goodman modifying factor described by Equation (2).

Looking at the range of the stresses in the conventional and modified adapters, it was decided that the results would be only compared to the endurance limit,  $S_{FL}$ . However, if at another particular case the stresses were to be higher, the SN curve for iron ductile 60-40-18 could be plotted, and the number of cycles calculated using a mathematical relationship. Results for the equivalent stresses can be found on the "Results and Discussion" Section.

## **FEA MODEL VALIDATION**

To obtain the fatigue life estimation of the bearing adapters, the work done by Montalvo et al. [3] needed to be expanded to the dynamic loading case. However, in order to use the developed finite element (FE) model, it was important to first validate the original FE model through a series of physical experiments. After validating the FE model, the model could be used to determine the stresses under dynamic loading and the number of operational cycles the bearing adapters would be able to withstand.

The purpose of the work presented here is to experimentally validate the FE model provided by Montalvo et al. [3]. The selected way to experimentally validate the finite element model is to compare the physical strain results of the bearing adapter to the FEA strain results in a simple loading scenario which produces the same levels of strain as the expected conditions. A physical experiment was done on an instrumented bearing adapter where the strain at a point of interest was measured using a strain gauge. Subsequently, the FE model was used in a linear stress FEA in order to replicate the physical experiment. Finally, the experimental and FEA (i.e. numerical) results were compared to determine the quality of the FE model.

### Instrumented Bearing Adapters

In order to expand the work done by Montalvo et al. [3] to the dynamic loading, the authors decided that the first step was to validate the finite element model with a physical experiment with instrumented conventional and modified adapters. The way this was done was by placing a full-bridge strain gauge at a point which would be convenient to compare results to the finite element analysis. The first logical position was to place the strain gauge at the top center of the adapter, since it had been determined as a point of interest in previous work. Therefore, it was decided to place the strain gauge at this location, in the cavity in the interface between the bearing adapter and the elastomer pad-liner, as shown in Figure 8.

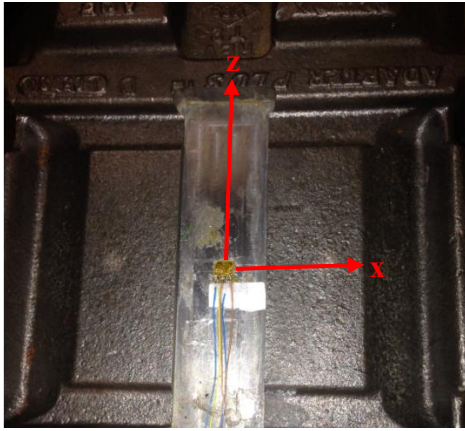


**Figure 8: Strain Gauge on Top of the Class K Bearing Adapter**

The strain gauge used is composed of a set of resistors as shown in Figure 9. The way the strain is obtained is by measuring difference in voltages before and after loading the component at which the strain gauge is placed. For this case, the voltage of individual resistors was measured to obtain the strain at different directions (e.g. x and z directions).

**Full-Bridge Circuit**

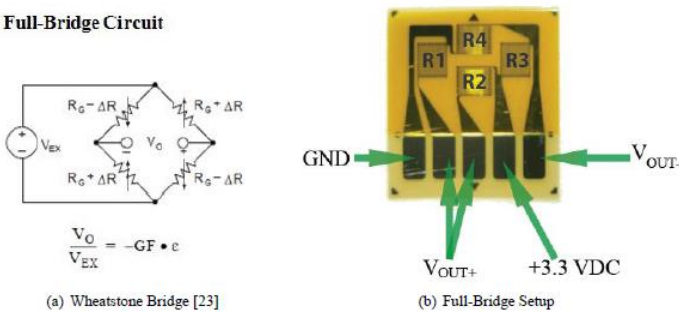


**Figure 9: Full-Bridge Strain Gauge**

In general, depending on how the component is loaded (e.g. bending, torsion, or axially) or the type of sensor (e.g. half-bridge, quarter-bridge), the strain can be calculated with a mathematical relationship followed by the procedures from National Instruments' *Measuring Strain with Strain Gauges* [6]. A voltage ratio was calculated and a strained gauge was obtained from the following equations

$$V_r = \left( \frac{V_{OUT}}{V_{IN}} \right)_{strained} - \left( \frac{V_{OUT}}{V_{IN}} \right)_{unstrained} \quad (6)$$

$$\epsilon = \frac{-4V_r}{GF(1+2V_r)} \times \left( 1 + \frac{R_l}{R_g} \right) \quad (7)$$

Where  $\epsilon$  is the measured strain, GF is the Gauge Factor,  $V_r$  is the voltage ratio,  $R_l$  is the lead resistance and  $R_g$  is the nominal gauge resistance.

**Experiment Setup: 4-Leg Support and Top Applied Pressure**

The bending experiment consisted of placing the four legs of the conventional and modified bearing adapters at a flat surface as shown in Figure 10 and Figure 11 and pressing

at the top with different compression loads. Approximate pressures of 300, 400, and 500 psi were applied at the top, which translate to loads of 1720, 2160 and 2600 lbs respectively. These loads produce strains that are in the same order of magnitude or larger than the experiments in Montalvo et al. [3]. During the experiment, the voltage change in the strain gauge was recorded at every loading time. After completing the experiments, the strain perceived by the adapter was calculated.



**Figure 10: Class K Bearing Adapter Test without Pad-Liner: 4-Leg Support and Top Applied Pressure**



**Figure 11: Class K Bearing Adapter Test with Pad-Liner: 4-Leg Support and Top Applied Pressure**

**Finite Element Analysis:**

A Finite Element Model that replicates the physical experiment (e.g. 4-Leg Support and Top Applied Pressure) was used in conjunction with ALGOR software. The model was discretized into approximately 90,000-300,000 elements with a mesh size of 0.1-0.2 in. for the adapter. The high range of number of elements was due to the convergence check of results. A combination of bricks, wedges, pyramids and tetrahedral elements were used to successfully mesh the model. A test of convergence was made in accordance with the work by Sinclair et al. [7] in order to check for accuracy of the results. The first boundary conditions applied to this model was that three of the legs of the adapter were prevented from moving in the vertical y-direction, while one of the legs was fixed in all directions, in order to simulate the adapter being in a flat surface. A surface pressure was then applied at the top

surface that translates into the force applied by the press. Results were recorded at the location of the strain gauge. The boundary conditions of the model are shown in Figures 12 and 13. Plots with the strain distribution are shown in Figure 14 and Figure 15.

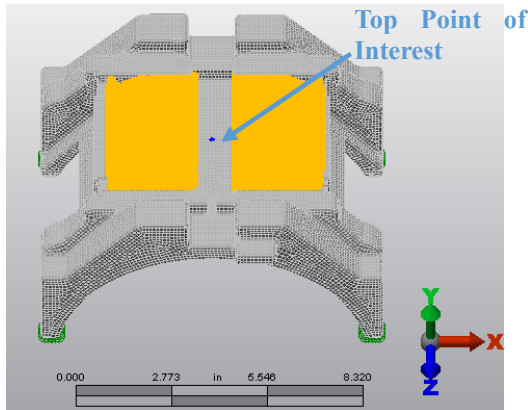


Figure 12: 4-Leg Support and Top Applied Pressure Finite Element Model (FEM)

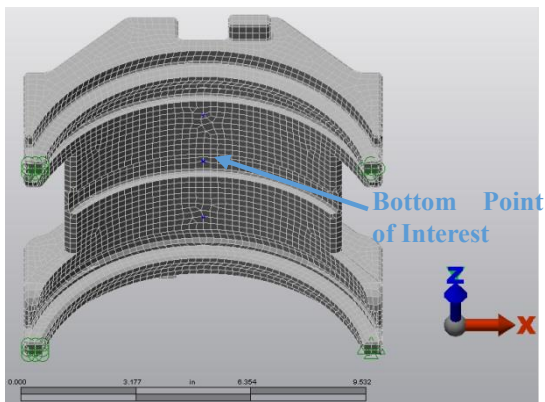


Figure 13: Class K Bearing Adapter FE Model with Bottom Point of Interest

## RESULTS AND DISCUSSION

It was of interest to validate the FEA results obtained previously by Montalvo et al [3]. In this section, the strain gauge results for the previously discussed model are presented along with the FEA strain distributions on the bearing adapter. Subsequently, one of the possible worst case scenarios is discussed and the previous FEA results by Montalvo et al. [3] are extended. Finally, an estimation of the operational life of the bearing adapters is made using the Stress-Life approach.

### FE Model Experimental Validation Results

Figures 14 and 15 show the strain distribution for the bearing adapter in the 4-Leg Support experiment. Tables 2 and 3 show the results obtained from the physical experiment and the finite element model for the conventional and modified bearing adapters. Even though the control of the load was done through a dial, the results show good matching between the experimental and the FEA results. The level of strains in these validation experiments are in the same order of magnitude or larger than the experiments in Montalvo et al. [3].

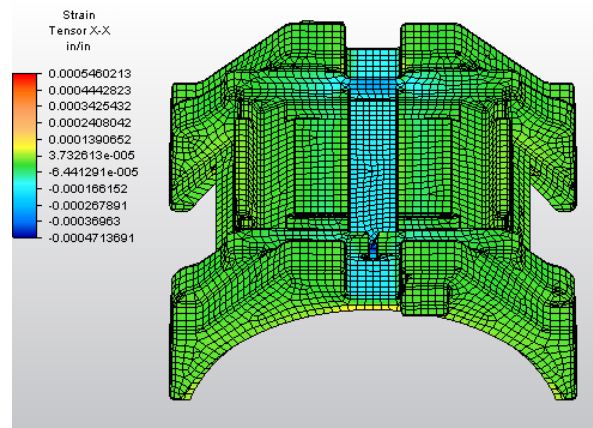


Figure 14: 4-Leg Support Strain Distribution

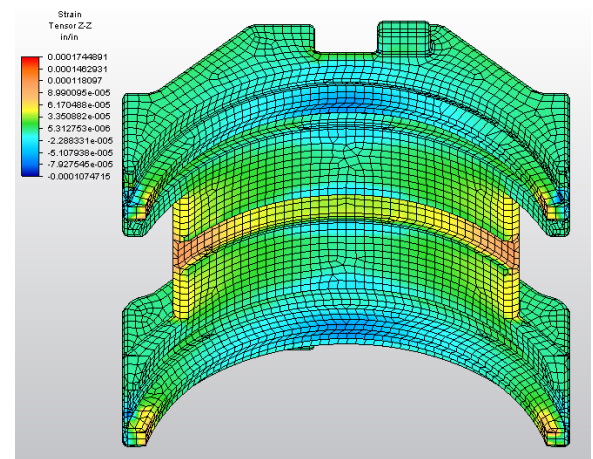


Figure 15: 4-Leg Support Strain Distribution

Table 2: Modified Adapter Testing and Validation  
x-direction

Load (lb)	Quarter Bridge,	Strain, FEA	Error
Axial Strain			
1,720	$-1.15 \times 10^{-4}$	$-1.15 \times 10^{-4}$	0%
2,160	$-1.43 \times 10^{-4}$	$-1.45 \times 10^{-4}$	1%
2,600	$-1.69 \times 10^{-4}$	$-1.74 \times 10^{-4}$	3%



**Table 3: Modified Adapter Testing and Validation**  
z-direction

Load (lb)	Quarter Bridge,	Strain, FEA	Error
Axial Strain			
<b>1,720</b>	$-2.93 \times 10^{-5}$	$-3.05 \times 10^{-5}$	4%
<b>2,160</b>	$-3.70 \times 10^{-5}$	$-3.83 \times 10^{-5}$	4%
<b>2,600</b>	$-4.39 \times 10^{-5}$	$-4.61 \times 10^{-5}$	5%

Fatigue Results

Tables 4-9 show the fatigue results for the conventional and modified bearing adapter at dynamic (impact) loading. The tables include the dynamic VM stress at the top of the adapter which was equal to the maximum stress on the fatigue estimation analysis. If the equivalent stress was below 24 ksi or the endurance limit, the bearing adapter was assumed to have infinite life. Looking at the results, one can see that all the stresses are below the endurance limit, which translates into having an infinite life. Therefore, it was determined that the original and modified adapters for onboard monitoring applications would not fail under the studied conditions.

**Table 4: Fatigue Results for Class K Original Adapter with Impact Uniform Distributed Load**

Contact Length	VM Stress on top center(ksi)	$S_{MAX}$ (ksi)	$S_{eq}$ (ksi)	Fatigue Life (cycles)
4 inch	5,966.53	5.97	<b>3.16</b>	Infinite
6 inch	6,320.77	6.32	<b>3.34</b>	Infinite

**Table 5: Fatigue Results for Class K Modified Adapter (0.05 in fillet) with Impact Uniform Distributed Load**

Contact Length	VM Stress on cutout edge(ksi)	$S_{MAX}$ (ksi)	$S_{eq}$ (ksi)	Fatigue Life (cycles)
4 inch	10,263.63	10.26	<b>5.61</b>	Infinite
6 inch	8,200.93	8.20	<b>4.40</b>	Infinite

**Table 6: Fatigue Results for Class K Modified Adapter (0.1 in fillet) with Impact Uniform Distributed Load**

Contact Length	VM Stress on cutout edge(ksi)	$S_{MAX}$ (ksi)	$S_{eq}$ (ksi)	Fatigue Life (cycles)
4 inch	9,101.40	9.10	<b>4.92</b>	Infinite
6 inch	8,503.50	8.50	<b>4.58</b>	Infinite

**Table 7: Fatigue Results for Class K Original Adapter with Impact Non-Uniform Distributed Load**

Contact Length	VM Stress on top center(ksi)	$S_{MAX}$ (ksi)	$S_{eq}$ (ksi)	Fatigue Life (cycles)
4 inch	6,024.36	6.02	<b>3.17</b>	Infinite
6 inch	6,949.13	6.95	<b>3.69</b>	Infinite

**Table 8: Fatigue Results for Class K Modified Adapter (0.05 in fillet) with Impact Non-Uniform Distributed Load**

Contact Length	VM Stress on cutout edge(ksi)	$S_{MAX}$ (ksi)	$S_{eq}$ (ksi)	Fatigue Life (cycles)
4 inch	16,715.68	16.72	<b>9.71</b>	Infinite
6 inch	11,761.45	11.76	<b>6.52</b>	Infinite

**Table 9: Fatigue Results for Class K Modified Adapter (0.1 in fillet) with Impact Non-Uniform Distributed Load**

Contact Length	VM Stress on cutout edge(psi)	$S_{MAX}$ (ksi)	$S_{eq}$ (ksi)	Fatigue Life (cycles)
4 inch	12677.64	12.68	7.09	Infinite
6 inch	11890.32	11.89	6.60	Infinite

**CONCLUSION**

Previous work conducted provided a finite element model for Class K Bearing Adapters. A continuation study determined that a possible worst case scenario for these components would be when the adapter is subjected to periodic dynamic loading such as a wheel impact load which translates into an equivalent static load of 90,000 lb on the bearing adapter. Stress distributions were obtained and analyzed under these conditions. In this paper, the fatigue life of conventional and modified bearing adapters were analyzed in order to determine the structural integrity of the adapter after material is removed. The method used to find the life was the Stress-life approach with Goodman correction factor. Equivalent stresses were determined, and it was found that conventional and modified adapters would have an infinite life at all studied loading conditions. Additional work is being performed to further validate the Finite Element model and to look at other worst case scenarios with loading conditions that may develop in the field through the operating life of the railroad track, the railcar truck assembly, and the railroad bearing.

**NOMENCLATURE**

SN	Stress-Life
$S_{FL}$	Fatigue Limit or Endurance Limit
$S_F$	Low Cycle Stress Value
$S_a$	Stress Amplitude, Alternating Stress Amplitude
$S_m$	Mean Stress
$S_{eq}$	Equivalent Stress
$S_{max}$	Maximum Stress
$S_{min}$	Minimum Stress
UTS	Ultimate Tensile Strength
$\rho$	Density
E	Modulus of Elasticity
$\nu$	Poisson’s ratio
$\epsilon$	Measured Strain

$V_r$	Voltage Ratio
GF	Gauge Factor
VM	Von Mises
$R_l$	Lead Resistance
$R_g$	Nominal Gauge Resistance

**ACKNOWLEDGMENTS**

This study was made possible by funding provided by the University Transportation Center for Railway Safety (UTCRS) through a USDOT Grant No. DTRT13-G-UTC59.

**REFERENCES**

- [1] Karunakaran, S., Snyder, T.W., “Bearing Temperature Performance in Freight Cars”, Proceedings of the ASME RTD 2007 Fall Technical Conference, Chicago, Illinois, September 11-12.
- [2] J. A. Kypuros, C. Tarawneh, A. Zagouris, S. Woods, B. M. Wilson, and A. Martin, “Implementation of wireless temperature sensors for continuous condition monitoring of railroad bearings”, Proceedings of the 2011 ASME RTD Fall Technical Conference, RTDF2011-67017, Minneapolis, Minnesota, September 21-22.
- [3] Montalvo, J., Trevino, A., Fuentes, A., Tarawneh, C., “Structural Integrity of Conventional and Modified Railroad Bearing Adapters for Onboard Monitoring”, Proceedings of the ASME 2014 International Mechanical Engineering Congress and Exposition, November 14-20, Montreal Canada.
- [4] Stratman, B., Liu, Y., Mahadevan, S., “Structural Health Monitoring of Railroad Wheels Using Wheel Impact Load Detectors,” J. Fail. Anal. And Preven., 7:218-225, 2007.
- [5] Stephens, R.I., Fatemi, A., Stephens, R.R., Fuchs, H.O., “Metal Fatigue in Engineering”, 2<sup>nd</sup> Edition, Wiley, 2000.
- [6] National Instruments, “Strain Gauge Configuration Types”, 2006. Online: <http://www.ni.com/white-paper/4172/en>.
- [7] Sinclair, G. B., “Practical Convergence-Divergence Checks for Stresses from FEA”, Proceedings of the 2006 International ANSYS Conference, Pittsburgh, PA.